



Published in final edited form as:

ACS Nano. 2012 September 25; 6(9): 8007–8014. doi:10.1021/nn302615f.

Antioxidant Carbon Particles Improve Cerebrovascular Dysfunction Following Traumatic Brain Injury

Brittany R. Bitner^{1,2,¶}, Daniela C. Marcano^{3,4,¶}, Jacob M. Berlin^{3,4,¶,‡}, Roderic H. Fabian^{5,6}, Leela Cherian⁵, James C. Culver², Mary E. Dickinson^{1,2}, Claudia S. Robertson⁵, Robia G. Pautler^{1,2}, Thomas A. Kent^{1,6,7}, and James M. Tour^{3,4}

¹Interdepartmental Program in Translational Biology and Molecular Medicine, Baylor College of Medicine, One Baylor Plaza, Houston, Texas, 77030, USA

²Department of Molecular Physiology and Biophysics, Baylor College of Medicine, One Baylor Plaza, Houston, Texas, 77030, USA

³Department of Chemistry, Rice University, MS-222, 6100 Main Street, Houston, Texas 77005, USA

⁴Smalley Institute for Nanoscale Science and Technology, Rice University, MS-222, 6100 Main Street, Houston, Texas 77005, USA

⁵Department of Neurosurgery and Baylor College of Medicine, One Baylor Plaza, Houston, Texas, 77030, USA

⁶Department of Neurology, Baylor College of Medicine, One Baylor Plaza, Houston, Texas, 77030, USA

⁷Michael E. DeBakey VA Medical Center, 2002 Holcombe Blvd, Houston, Texas 77030, USA.

Abstract

Injury to the neurovasculature is a feature of brain injury and must be addressed to maximize opportunity for improvement. Cerebrovascular dysfunction, manifested by reduction in cerebral blood flow (CBF), is a key factor that worsens outcome after traumatic brain injury (TBI), most notably under conditions of hypotension. We report here that a new class of antioxidants, poly(ethylene glycol)-functionalized hydrophilic carbon clusters (PEG-HCCs), which are nontoxic carbon particles, rapidly restore CBF in a mild TBI/hypotension/resuscitation rat model when administered during resuscitation—a clinically relevant time point. Along with restoration of CBF, there is a concomitant normalization of superoxide and nitric oxide levels. Given the role of poor CBF in determining outcome, this finding is of major importance for improving patient health under clinically relevant conditions during resuscitative care and it has direct implications for the current TBI/hypotension war-fighter victims in the Afghanistan and Middle East theaters. The results also have relevancy in other related acute circumstances such as stroke and organ transplantation.

Correspondence to: Thomas A. Kent; James M. Tour.

Corresponding Authors: tkent@bcm.edu, tour@rice.edu.

[‡]Present address: Department of Molecular Medicine, The Beckman Research Institute of the City of Hope, Duarte, California, USA.

[¶]These authors contributed equally.

Supporting Information Available. Additional images, graphs, data and tables. This material is available free of charge *via* the Internet at <http://pubs.acs.org>.

Keywords

traumatic brain injury; cerebral blood flow; antioxidants; hydrophilic carbon clusters; nanoparticles

The neurovascular unit, composed of neuronal and non-neuronal cells such as vascular cells, comprise an integrated network responsible for important physiological functions in the brain including regulation of blood flow.¹ The brain has a high metabolic demand that is met by maintenance of cerebral blood flow (CBF) even under conditions of altered systemic blood pressure, a process termed cerebral autoregulation.² It is achieved by the ability of the brain vasculature to dilate in the face of low blood pressure and constrict during increased blood pressure in order to maintain its perfusion within physiological range. Loss of autoregulation can expose the brain to hypoperfusion during low blood pressure (hypotension) and to excess blood flow and potentially bleeding during high blood pressure (hypertension). Dysfunction of the neurovascular unit is recognized as a major determinant of patient outcome after brain injury, and it has been hypothesized that therapies that do not address that dysfunction are unlikely to promote recovery.¹ In the case of traumatic brain injury (TBI), damage to the neurovascular unit is manifested under conditions of abnormally low blood pressure, known as hypotension, by loss of cerebral autoregulation and poor restoration of blood flow even after treatment with fluids to increase blood pressure (resuscitation).³ Loss of autoregulation and poor reperfusion contribute to the clinical finding that TBI with a secondary insult of hypotension predicts poor outcome.⁴ This poor outcome is seen even when the brain injury is classified as mild TBI, more commonly known as a concussion. Elevated levels of reactive oxygen species (ROS) such as superoxide (SO)^{5,6} are found in the vasculature and have been shown to mediate loss of autoregulatory tone. Along with spikes of ROS following trauma, continued damaging spikes in the level of ROS are observed upon subsequent blood reinfusion during resuscitation;⁷ hence, in an effort to stabilize the patient, furtherance of oxidative damage ensues.^{8,9} However, blood reinfusion also provides an opportunity to intervene at a clinically realistic time point.

A variety of functionalized carbon materials such as single-walled carbon nanotubes, multi-walled carbon nanotubes, graphene, fullerenes, and/or their derivatives have been studied for the treatment of many diseases, including cancer,¹⁰⁻¹² arthritis,¹³⁻¹⁵ inflammation,¹⁶ and neurodegenerative¹⁷⁻¹⁹ diseases. In this report we demonstrate that poly(ethylene glycol)-functionalized hydrophilic carbon clusters (PEG-HCCs), which are nontoxic carbon particles, rapidly restore cerebral blood flow (CBF) in a TBI/hypotension/resuscitation rat model when administered during resuscitation. Remarkably, along with restoration of CBF, there is a concomitant normalization of both SO and the vasodilator, nitric oxide (NO), levels.

There are currently no antioxidants, including PEG-superoxide dismutase (PEG-SOD) and tirilizad, which have improved patient outcome following TBI.²⁰ One reason for the lack of effectiveness could be due to the mechanism by which antioxidants trap radicals. Many of these agents modify the radical and depend on the presence of additional detoxifying molecules, such as catalase or glutathione to regenerate the antioxidant.²⁰ Unfortunately, in the toxic post-injury environment, these downstream molecules are depleted and cannot sufficiently detoxify the damaging radicals. Other agents, such as Vitamin E, are insufficiently regenerated in the face of rising levels of oxidative radicals.²¹ While it is probably not possible to administer therapy in time to avert the initial instantaneous spike in ROS following TBI, it should be possible to include an antioxidant at the time of resuscitation and reperfusion to avert the subsequent waves of damaging ROS and their

damaging cascades. Therefore, a useful clinical agent would need to act rapidly *in vivo* following the release of the ROS, have high capacity for radical annihilation where there is no need for complementary detoxifying molecules, and it should be effective at a clinically realistic time point such as during the resuscitation.

Particle-based systems are an emerging class of antioxidants with potential advantages over currently available antioxidants²²⁻³¹ due to the possibility that they can fully quench radicals without the need for assistance from other detoxifying molecules, as in the case of superoxide dismutase, for example.³² HCCs are chemically cut carbon materials, 30- to 40-nm-long and 2- to 3-nm wide, possessing both graphitic and oxidized domains, the latter being the addend locations for PEGylation *via* amide linkages.³³ PEG-HCCs are *in vitro* antioxidants,³⁴ and they can also be non-covalently loaded with hydrophobic drugs for *in vivo* delivery.³³ PEG-HCCs have the hydrodynamic volume of a moderately sized protein; hence, they are diminutive. Dynamic light scattering (DLS) measurements indicate that they are 50 nm in size at neutral pH.³³ Preliminary studies that used histological analysis of major organs along with hematology measurements demonstrated that the PEG-HCCs have no acute toxicity, and a biodistribution study indicated that they were primarily cleared through the kidneys with a blood half-life of 2 to 3 h.³³ Finally, PEG-HCCs are room-temperature stable for months, biocompatible with cultured brain endothelial cells (bEnd.3), and they can be targeted with monoclonal antibodies, such as P-selectin, to specific cellular locations on tissue of interest.^{34,35}

It is conjectured that PEG-HCCs' graphitic structural domains cause them to be antioxidants by radical annihilation (Figure 1) rather than by radical transfer to a less reactive radical form as is required for most other antioxidants. Thus, PEG-HCCs can detoxify many radicals at each of their graphitic domains, as demonstrated by our previous finding that PEGHCCs are potent antioxidants after generation of SO, one of the damaging ROS overproduced during TBI.³⁴ It is thus possible that *in vivo* the PEG-HCCs can annihilate toxic ROS during periods of trauma when other antioxidants are overwhelmed due to a lack of supporting detoxifying molecules. Hence, PEG-HCCs alone may function as effective antioxidants and have sufficient capacity for radical annihilation to be used therapeutically during periods of intense ROS generation. These multifaceted properties suggest that the PEG-HCCs could be exciting constructs for clinical evaluation.

Results

First, by confocal microscopy studies, we confirmed that the PEG-HCCs are rapidly internalized by murine brain endothelial (b.End3) cells (Methods and Figure S1-S3). Brain endothelial cells were chosen because, as discussed, the vasculature is a major and potentially treatable injury in the TBI and secondary injury paradigm that results in loss of autoregulation.^{3,5} A series of *in vitro* studies showed that when oxidative stress was induced in b.End.3 cells³⁶ by treatment with the mitochondrial toxin, antimycin A,^{22,25,34,37} the intracellular oxidative stress could be reduced in a dose-dependent manner by treatment with PEG-HCCs. Antimycin A blocks electron flow through complex III of the mitochondrial electron transport chain that results in the formation of SO.³⁷ The amount of oxidative radical expression was measured as a proportion of dihydroethidium (DHE) fluorescence.³⁸ PEG-HCC treatment was effective even 10 min after toxin exposure, while neither PEG-SOD nor the small molecule antioxidant, phenyl- α -*tert*-butyl nitron (PBN)^{7,39,40} was effective in the post-toxin-treated cells. The latter two traditional antioxidants were only effective pre-toxin exposure, and then only at a 10 to 30 \times higher dose (Figure 2A). Furthermore, at higher doses of antimycin A where significant cell death could be induced, post-treatment with PEG-HCCs was able to restore cell viability to more than 65% of baseline. Conversely, no protective effect from post-treatment with either PEGSOD or PBN

could be observed (Figure 2B). These studies underscore the efficacy of the PEGHCCs to annihilate ROS that would otherwise have resulted in cell death; the poor performance of conventional antioxidants is also noted.

Furthermore, it was found that PEG-HCCs are selective antioxidants as additional *in vitro* experiments in bEnd.3 cells indicated that the PEG-HCCs do not quench NO sensitive fluorescence of diaminofluorescein diacetate (DAF-2DA)⁴⁰ associated with spontaneous NO release from these cells (Figures S4-S5). This may be significant for eventual clinical efficacy since physiological levels of NO are essential for many processes, including blood vessel dilation and autoregulation.⁴¹ An effective antioxidant treatment for TBI must annihilate toxic species such as SO without impairing the normal levels and functions of NO.

PEG-HCCs were next evaluated *in vivo*. The TBI model used here is intended to mimic the common clinical situation in which TBI is accompanied by a systemic injury resulting in hypotension (low blood pressure). There is minimal evidence of either behavioral or histological injury with either TBI or hypotension alone, but with the superimposition of hemorrhagic hypotension and subsequent resuscitation, there is marked expansion of lesion size and behavioral impairment (Figure S6).⁴² Reperfusion CBF was reduced in proportion to the increase in injury, supporting the hypothesis that this is primarily a vasculature injury. The loss of autoregulation and poor reperfusion originating in the brain endothelium contribute to injury even in the setting of mild TBI. This highlights that while the blood-brain barrier becomes compromised following mild TBI⁴³ potentially allowing access of agents such as PEG-HCCs to the brain itself, the major treatable injury in the TBI and secondary injury paradigm is to the brain vasculature manifested by loss of CBF and poor reperfusion.

Using this TBI/hypotension/resuscitation rat model, treatment was chosen to simulate a typical case in the field: 50 min after controlled cortical impact TBI and loss of blood, lactated Ringers solution was administered in an ambulance “prehospital” phase, then after further delay of 30 min, definitive “hospital” care consisted of therapy administration, oxygenation and blood infusion. The model is outlined in the Injury Model Table 1 and described as follows: In Phase 1, Long Evans rats (250 to 300 g) underwent sham injury or mild cortical compression injury TBI (3 m/s, 2.5 mm deformation, Table S1) to one hemisphere of the brain. Sham animals underwent identical surgical preparation as the TBI group except they did not receive the cortical impact used to produce mild TBI. Both sham and mild TBI animals had hemorrhagic hypotension produced by controlled blood withdrawal to reach a mean arterial blood pressure (MAP) of 40 mm Hg in a decelerating protocol to mimic trauma blood loss. In order to simulate field resuscitation and ambulance transport (Phase 2), the rats received intravenous (i.v.) lactated Ringer's solution for initial resuscitation. Then hospital care (Phase 3) was simulated by administering a single dose of PEG-HCCs (2 mg/kg) or a diluent vehicle, phosphate buffered saline (PBS), *via* a 5 min i.v. tail vein administration. This was followed by oxygenation and blood reinfusion. Beginning with Phase 4, there was extensive physiological monitoring included MAP, arterial blood gases, intracranial pressure and non-invasive spatial brain perfusion using laser Doppler flowmetry (LDF, Periscan).⁴²

Results and Discussion

Remarkably, PEG-HCCs restored cerebral perfusion and normalized the oxidative radical profile. Rats received a single dose of PEG-HCCs (2 mg/kg) or PBS at the beginning of the blood resuscitation (Phase 3). CBF was measured for 6 h from the brain surface with LDF (Phases 3 and 4). Just before the 6 h mark, rats were injected with dyes for SO (DHE) and

NO (DAF-2DA) detection, and perfusion fixed.⁴⁰ Systemic injection of these dyes and a short circulation time was able to identify vascular expression of these radicals since the dyes are concentrated in the vasculature with less chance of diffusion into the brain parenchyma.⁴⁰ LDF-relative CBF (rCBF) is shown in the series of Figures 3A-C. Figure 3A illustrates changes in rCBF in the region of the traumatic injury. Hypotension following TBI significantly reduced rCBF. In the vehicle-treated TBI group, rCBF was only partially restored by reinfusion of shed blood while rCBF returned rapidly to baseline levels following administration of the PEG-HCCs and blood. The duration of the PEG-HCC effect was from 2 to 3 h, at which time both groups showed a decline in rCBF; this duration of treatment effect is consistent with the 2 to 3 h blood half-life of PEG-HCCs³³ and also consistent with the prolonged anesthesia time. Figure 3B shows a qualitatively similar effect in the peri-traumatic region (region around the injury), with rCBF returning to baseline in the PEG-HCC-treated group, while remaining depressed in the vehicle-treated group. No effect on rCBF of either group in the contralateral cortex (Figure 3C) indicates that the outcomes seen in the lesion and peri-lesional regions were not artifactual and were specific for injured areas. Additional experiments in a model to simulate linear flow show that there was no effect of PEG-HCCs on the LDF signal used to measure CBF, nor did the PEGHCCs influence systemic blood pressure or physiological variables (Figure S7, Table S2). These results demonstrated that in a model of TBI/hypotension/resuscitation, the PEG-HCCs rapidly restore the cerebral perfusion and that the PEG-HCCs were directly improving CBF in the injured area.

We next determined whether treatment was able to modify the hypothesized targets, SO while restoring NO. The injection of PEG-HCC antioxidants significantly reduced SO levels in the vasculature (Figures 4A-C), underscoring that this is primarily a vasculature injury. Concomitantly, treatment with PEG-HCCs completely restores vascular NO levels (Figures 4D F). This duality of modes in the resuscitative phase of treatment, specifically decreasing SO and normalizing NO, is highly unusual in such injury models.

Conclusions

Non-toxic PEG-HCCs are inherently active particle-based drugs that have efficacy at the critical neurovascular unit, restoring CBF after a mild TBI. Since reduction in CBF following even mild TBI is a major cause of poor outcome, the results shown for restoring CBF while normalizing SO and NO levels primarily in the cerebral vasculature are suggestive of a treatment that could vastly improve the recovery and long-term neurological prognosis for traumatized patients, and it has implications for other acute disorders such as stroke in which reperfusion-based ROS release is associated with extension and propagation of injury.⁷

Methods

PEG-HCCs were prepared as previously described.³³ These particles are soluble in water and PBS. Optical spectrum (Figure S8A), thermogravimetric analysis (TGA, Figure S8B), and X-ray photoelectron spectroscopy (XPS, Figure S8C) measurements were consistent with the previously reported³³ characterization of these materials. According to the TGA, the PEG-HCCs used in the current studies were 84% PEG by weight.

DAF-2DA staining in bEnd.3 cells: bEnd.3 cells (ATCC) were grown in Dulbecco's modified Eagle's medium (4 mM L-glutamine adjusted to contain 1.5 g/L sodium bicarbonate and 4.5 g/L glucose, 90%; fetal bovine serum, 10% (Atlanta Biological) in an incubator set to 37 °C with 5% CO₂. Aliquots of 60,000 cells in 0.5 mL were added directly onto sterile 25 mm round cover glasses inside 6 well plates. The cells were allowed to attach

for 15 min after which an additional 1.5 mL of media was added and then the cells were placed in an incubator and allowed to grow for 48 h. PEG-HCCs were added to each well to obtain the following concentrations: 0 mg/L, 0.1 mg/L, 1 mg/L, 10 mg/L, 20 mg/L and 30 mg/L (triplicate). The cells were incubated for 1 h with the specific PEG-HCC concentrations after which DAF-2DA at a final concentration of 5 mM was added to each well and incubated for an additional 5 min. The cells were then washed 3× with PBS and fixed with 4% paraformaldehyde for 15 min. The cells were washed 3× with PBS and then the cover glasses were attached to glass slides and coverslipped. A Nikon eclipse 80i microscope set to FITC was used to capture ten 40X fields per slide. Five cells from each 40X field were analyzed using NIS Elements software. An auto detect region of interest (ROI) function was used to select the cells and calculate their mean intensity and area. The intensity/area/exposure was calculated. An ANOVA was performed using the means followed by post tests using the Bonferroni method.

Confocal microscopy showed that the PEG-HCCs were taken up by the endothelial cells (Figure 1S and 3S). Staining against the PEG for the mock (Figure 1S-B) and PEG (Figure 1S-E) treated cells showed similar low intensity signals, indicating that uptake was dependent on the presence of carbon particles but not the PEG. The experiment was set as follow: bEnd.3 cells (~50,000/well, passage less than 30 times) were grown on coverslips placed in 6-well plates with 5 mL of complete media (high glucose Dulbecco's modified Eagle's medium (Gibco) formulated to contain 4 mM L-glutamine, 3.7 g/L sodium bicarbonate, 4.5 g/L D-glucose, 1 mM sodium pyruvate, 90%; fetal bovine serum, 10%; 1× pen-strep). Cells were later treated with 5 mL of complete medium in a 1:1 mixture with water (Mock treatment), a solution of PEG in water, or a solution of PEG-HCCs in water. The final concentration of the PEG and PEG-HCCs in the treatment solution was 4 mg/L. Cells were incubated at 37 °C with 5% CO₂ for 5.5 h. The cells were then washed with ice cold PBS, then a solution of glycine (50 mM)/NaCl (100 mM), followed again by ice cold PBS in order to remove the carbon particles that are weakly attached to the membrane. Cells were fixed with 4% paraformaldehyde, then cell membranes were stained with Wheat Germ Agglutinin 594 before being permeabilized with PBT (PBS containing 0.1% Triton X-100), blocked with 5% BSA in PBT, and immunostained with a primary antibody against PEG (Epitomics, PEG Rabbit Monoclonal Antibody, RabMAb® #: 2061-1) and an Alexa-633 conjugated secondary antibody, with DAPI used as a nuclear counterstain. Each set of images was taken with the same settings on a Zeiss LSM 510 META confocal microscope, and are shown at the same brightness/contrast levels.

Supplementary Material

Refer to Web version on PubMed Central for supplementary material.

Acknowledgments

Funding was provided by the Mission Connect Mild Traumatic Brain Injury Consortium, funded by the Department of Defense: W81XWH-08-2-0141, W81XWH-08-2-0143 and W81XWH-08-2-0132. We also thank the support of the Alliance for NanoHealth through a subcontract from the University of Texas Health Science Center, Houston (Department of Defense: W8XWH-07-2-0101); Nanoscale Science and Engineering Initiative of the National Science Foundation under NSF Award EEC-0647452 for funding through the NSF Center for Biological and Environmental Nanotechnology; the Graduate Fellows in K-12 education at Baylor College of Medicine, funded by the National Science Foundation (Track 2, 0440525); the BCM DERC Pilot and Feasibility Award (P30DK079638-02); NIH R01 HL095586; the BCM Cytometry and Cell Sorting Core with funding from the NIH (NCR grant S10RR024574, NIAID AI036211 and NCI P30CA125123); and an NIH Training Grant from the National Heart, Lung, and Blood Institute (T32 HL007676).

References

1. Lo EH. Experimental Models, Neurovascular Mechanisms and Translational Issues in Stroke Research. *Br. J. Pharmacol.* 2008; 88:S396–S405. [PubMed: 18157168]
2. Paulson OB, Strandgaard S, Edvinsson L. Cerebral Autoregulation. *Cerebrovasc. Brain. Metab. Rev.* 1990; 2:161–192. [PubMed: 2201348]
3. DeWitt DS, Prough DS. Traumatic Cerebral Vascular Injury: the Effects of Concussive Brain Injury on the Cerebral Vasculature. *J. Neurotrauma.* 2003; 20:795–825. [PubMed: 14577860]
4. Butcher I, Maas AI, Lu J, Marmarou A, Murray GD, Mushkudiani NA, McHugh GS, Steyerberg EW. Prognostic Value of Admission Blood Pressure in Traumatic Brain Injury: Results from the IMPACT Study. *J. Neurotrauma.* 2007; 24:294–302. [PubMed: 17375994]
5. Kontos HA, Wei EP. Superoxide Production in Experimental Brain Injury. *J. Neurosurg.* 1986; 64:803–807. [PubMed: 3009736]
6. Kehrer JP. Free Radicals as Mediators of Tissue Injury and Disease. *Crit. Rev. Toxicol.* 1993; 23:21–48. [PubMed: 8471159]
7. Fabian RH, DeWitt DS, Kent TA. *In Vivo* Detection of Superoxide Anion Production by the Brain Using a Cytochrome c Electrode. *J. Cereb. Blood Flow Metab.* 1995; 15:242–247. [PubMed: 7860658]
8. Halliwell, B.; Gutteridge, JMC., editors. *Free Radicals in Biology and Medicine.* Oxford University Press; Oxford, New York: 1999. p. xxxi-936.
9. Ansari MA, Roberts KN, Scheff SW. A Time Course of Contusion-Induced Oxidative Stress and Synaptic Proteins in Cortex in a Rat Model of TBI. *J. Neurotrauma.* 2008; 25:513–526. [PubMed: 18533843]
10. Murakami T, Sawada H, Tamura G, Yudasaka M, Iijima S, Tasuchida K. Water-Dispersed Single-Wall Carbon Nanohorns as Drug Carriers for Local Cancer Chemotherapy. *Nanomedicine.* 2008; 3:453–463. [PubMed: 18694307]
11. Hampel S, Kunze D, Haase D, Krämer K, Rauschenback M, Ritschel M, Leonhardt A, Thomas J, Oswald S, Hoffmann V, et al. Carbon Nanotubes Filled With a Chemotherapeutic Agent: a Nanocarrier Mediates Inhibition of Tumor Cell Growth. *Nanomedicine.* 2008; 3:175–182. [PubMed: 18373424]
12. Liu Z, Robinson JT, Sun X, Dai H. PEGylated Nanographene Oxide for Delivery of Water-Insoluble Cancer Drugs. *J. Am. Chem. Soc.* 2008; 130:10876–10877. [PubMed: 18661992]
13. Yudoh K, Karasawa R, Masuko K, Kato T. Water-Soluble Fullerene (C₆₀) Inhibits the Development of Arthritis in the Rat Model of Arthritis. *Int. J. Nanomedicine.* 2009; 4:217–225. [PubMed: 19918368]
14. Nakamura M, Tahara T, Ikehara Y, Murakami T, Tsuchida K, Iijima S, Waga I, Yudasaka M. Single-walled Carbon Nanohorns as Drug Carriers: Adsorption of Prednisolone and Anti-Inflammatory Effects on Arthritis. *Nanotechnology.* 2011; 22:465102. [PubMed: 22024636]
15. Girase B, Shah J, Misra RD. Cellular Mechanics of Modulated Osteoblasts Functions in Graphene Oxide Reinforced Elastomers. *Adv. Eng. Mater.* 2012; 14:B101–B111.
16. Huang S, Ho C, Lin C, Fang H, Peng Y. Development and Biological Evaluation of C₆₀ Fulleropyrrolidine-Thalidomide Dyad as a New Anti-Inflammation Agent. *Bioorg. Med. Chem.* 2008; 16:8619–8626. [PubMed: 18723357]
17. Makarova EG, Gordon RY, Podolski IY. Fullerene C₆₀ Prevents Neurotoxicity Induced by Intrahippocampal Microinjection of Amyloid- β Peptide. *J. Nanosci. Nanotechnol.* 2012; 12:119–126. [PubMed: 22523954]
18. Zhang Y, Bai Y, Yan B. Functionalized Carbon Nanotubes for Potential Medicinal Applications. *Drug Discov. Today.* 2010; 15:428–435. [PubMed: 20451656]
19. Lv M, Zhang Y, Liang L, Wei M, Hu W, Li X, Huang Q. Effect of Graphene Oxide on Undifferentiated and Retinoic Acid-Differentiated SH-SY5Y Cells Line. *Nanoscale.* 2012; 4:3861. [PubMed: 22653613]
20. Muizelaar JP, Marmarou A, Young HF, Choi SC, Wolf A, Schneider RL, Kontos HA. Improving the Outcome of Severe Head Injury with the Oxygen Radical Scavenger Polyethylene Glycol-

- Conjugated Superoxide Dismutase: a Phase II trial. *J. Neurosurg.* 1993; 78:375–382. [PubMed: 8433137]
21. Wang X, Quinn PJ. Vitamin E and its Function in Membranes. *Prog. Lipid Res.* 1999; 38:309–336. [PubMed: 10793887]
 22. Lucente-Schultz RM, Moore VC, Leonard AD, Price BK, Kosynkin DV, Lu M, Partha R, Conyers JL, Tour JM. Antioxidant Single-Walled Carbon Nanotubes. *J. Am. Chem. Soc.* 2009; 131:3934–3941. [PubMed: 19243186]
 23. Ali SS, Hardt JI, Dugan LL. SOD Activity of Carboxyfullerenes Predicts Their Neuroprotective Efficacy: a Structure-Activity Study. *Nanomedicine:UK.* 2008; 4:283–294.
 24. Ali SS, Hardt JI, Quick KL, Kim-Han JS, Erlanger BF, Huang TT, Epstein CJ, Dugan LL. A Biologically Effective Fullerene (C60) Derivative with Superoxide Dismutase Mimetic Properties. *Free Radic. Biol. Med.* 2004; 37:1191–1202. [PubMed: 15451059]
 25. Dugan LL, Lovett EG, Quick KL, Lotharius J, Lin TT, O'Malley KL. Fullerene-Based Antioxidants and Neurodegenerative Disorders. *Parkinsonism Relat. Disord.* 2001; 7:243–246. [PubMed: 11331193]
 26. Dugan LL, Turetsky DM, Du C, Lobner D, Wheeler M, Almli CR, Shen CK, Luh TY, Choi DW, Lin TS. Carboxyfullerenes as Neuroprotective Agents. *Proc. Natl. Acad. Sci.* 1997; 94:9434–9439. [PubMed: 9256500]
 27. Quick KL, Ali SS, Arch R, Xiong C, Wozniak D, Dugan LL. A Carboxyfullerene SOD Mimetic Improves Cognition and Extends the Lifespan of Mice. *Neurobiol. Aging.* 2008; 29:117–128. [PubMed: 17079053]
 28. Das M, Patil S, Bhargava N, Kang JF, Riedel LM, Seal S, Hickman JJ. Auto-Catalytic Ceria Nanoparticles Offer Neuroprotection to Adult Rat Spinal Cord Neurons. *Biomaterials.* 2007; 28:1918–1925. [PubMed: 17222903]
 29. Hirst SM, Karakoti AS, Tyler RD, Sriranganathan N, Seal S, Reilly CM. Anti-Inflammatory Properties of Cerium Oxide Nanoparticles. *Small.* 2009; 5:2848–2856. [PubMed: 19802857]
 30. Schubert D, Dargusch R, Raitano J, Chan SW. Cerium and Yttrium Oxide Nanoparticles are Neuroprotective. *Biochem. Biophys. Res. Commun.* 2006; 342:86–91. [PubMed: 16480682]
 31. Martín R, Menchón C, Apostolova N, Victor VM, Alvaro M, Herance JR, García H. Nano-Jewels in Biology. Gold and Platinum on Diamond Nanoparticles as Antioxidant Systems Against Cellular Oxidative Stress. *ACS Nano.* 2010; 4:6957–6965. [PubMed: 20939514]
 32. McCord JM, Fridovich I. Superoxide Dismutase. An Enzymic Function for Erythrocyte (Hemocyte). *J. Biol. Chem.* 1969; 244:6049–6055. [PubMed: 5389100]
 33. Berlin JM, Leonard AD, Pham TT, Sano D, Marcano DC, Yan S, Fiorentino S, Milas ZL, Kosynkin DV, Price BK, et al. Effective Drug Delivery, *In Vitro* and *In Vivo*, by Carbon-Based Nanovectors Noncovalently Loaded with Unmodified Paclitaxel. *ACS Nano.* 2010; 4:4621–4636. [PubMed: 20681596]
 34. Marcano DC, Bitner BR, Berlin JM, Jarjoura J, Lee JM, Jacob A, Fabian RH, Kent TA, Tour JM. Design of Poly(ethylene glycol)-Functionalized Hydrophilic Carbon Clusters for Targeted Therapy of Cerebrovascular Dysfunction in Mild Traumatic Brain Injury. *J. Neurotrauma.* in press.
 35. Sano D, Berlin JM, Pham TT, Marcano DC, Valdecanas DR, Zhou G, Milas L, Myers JN, Tour JM. Noncovalent Assembly of Targeted Carbon Nanovectors Enables Synergistic Drug and Radiation Cancer Therapy *In Vivo*. *ACS Nano.* 2012; 6:2497–2505. [PubMed: 22316245]
 36. Montesano R, Pepper MS, Möhle-Steinlein U, Risau W, Wagner EF, Orci L. Increased Proteolytic Activity is Responsible for the Aberrant Morphogenetic Behavior of Endothelial Cells Expressing the Middle T Oncogene. *Cell.* 1990; 62:435–445. [PubMed: 2379237]
 37. Han D, Williams E, Cadenas E. Mitochondrial Respiratory Chain-Dependent Generation of Superoxide Anion and Its Release into the Intermembrane Space. *Biochem. J.* 2001; 353:411–416. [PubMed: 11139407]
 38. Aykin-Burns N, Ahmad IM, Zhu Y, Oberley LW, Spitz DR. Increased Levels of Superoxide and H₂O₂ Mediate the Differential Susceptibility of Cancer Cells Versus Normal Cells to Glucose Deprivation. *Biochem. J.* 2009; 418:29–37. [PubMed: 18937644]

39. Marklund N, Lewander T, Clausen F, Hillered L. Effects of the Nitron Radical Scavengers PBN and S-PBN on *In Vivo* Trapping of Reactive Oxygen Species After Traumatic Brain Injury in Rats. *J. Cereb. Blood Flow Metab.* 2001; 21:1259–1267. [PubMed: 11702041]
40. Fabian RH, Perez-Polo JR, Kent TA. Perivascular Nitric Oxide and Superoxide in Neonatal Cerebral Hypoxia-Ischemia. *Am. J. Physiol. Heart. Circ. Physiol.* 2008; 295:H1809–H1814.
41. Toda N, Ayajiki K, Okamura T. Cerebral Blood Flow Regulation by Nitric Oxide: Recent Advances. *Pharmacol. Rev.* 2009; 61:62–97. [PubMed: 19293146]
42. Navarro JC, Pillai S, Cherian L, Garcia R, Grill RJ, Robertson CS. Histopathological and Behavioral Effects of Immediate and Delayed Hemorrhagic Shock After Mild Traumatic Brain Injury in Rats. *J. Neurotrauma.* 2012; 29:322–334. [PubMed: 22077317]
43. Hicks RR, Smith DH, Lowenstein DH, Saint Marie R, McIntosh TK. Mild Experimental Brain Injury in the Rat Induces Cognitive Deficits Associated with Regional Neuronal Loss in the Hippocampus. *J. Neurotrauma.* 1993; 10:405–414. [PubMed: 8145264]

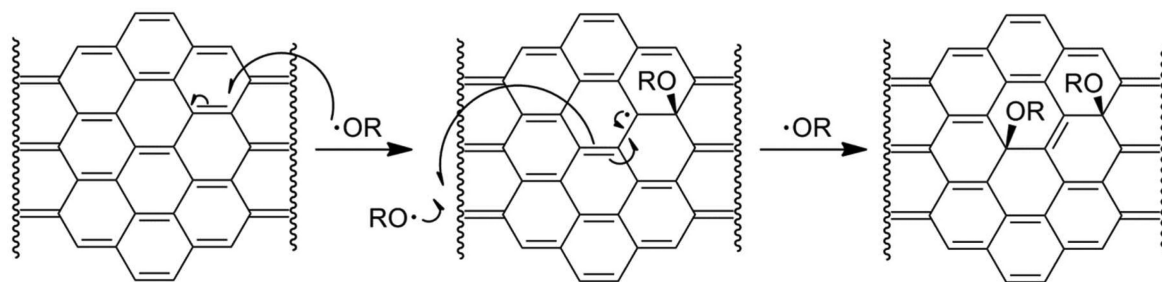
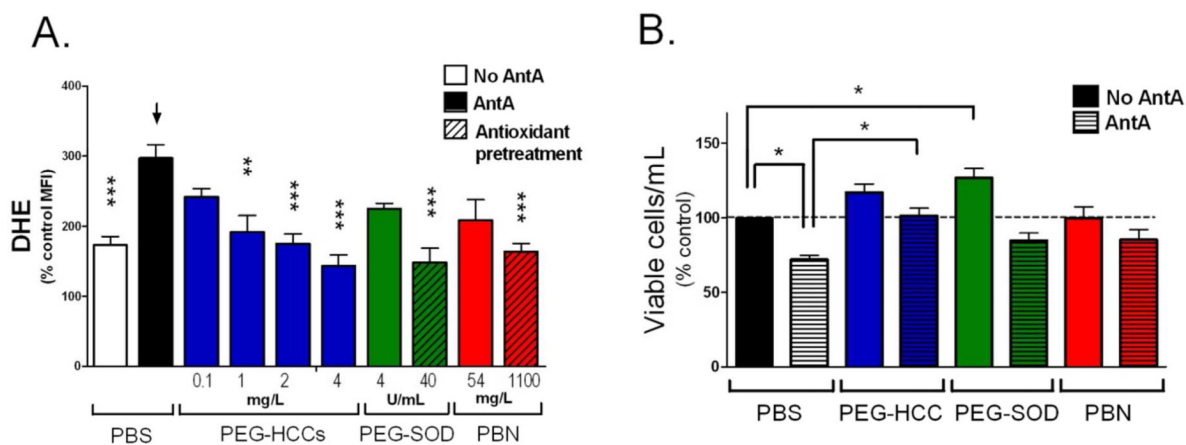
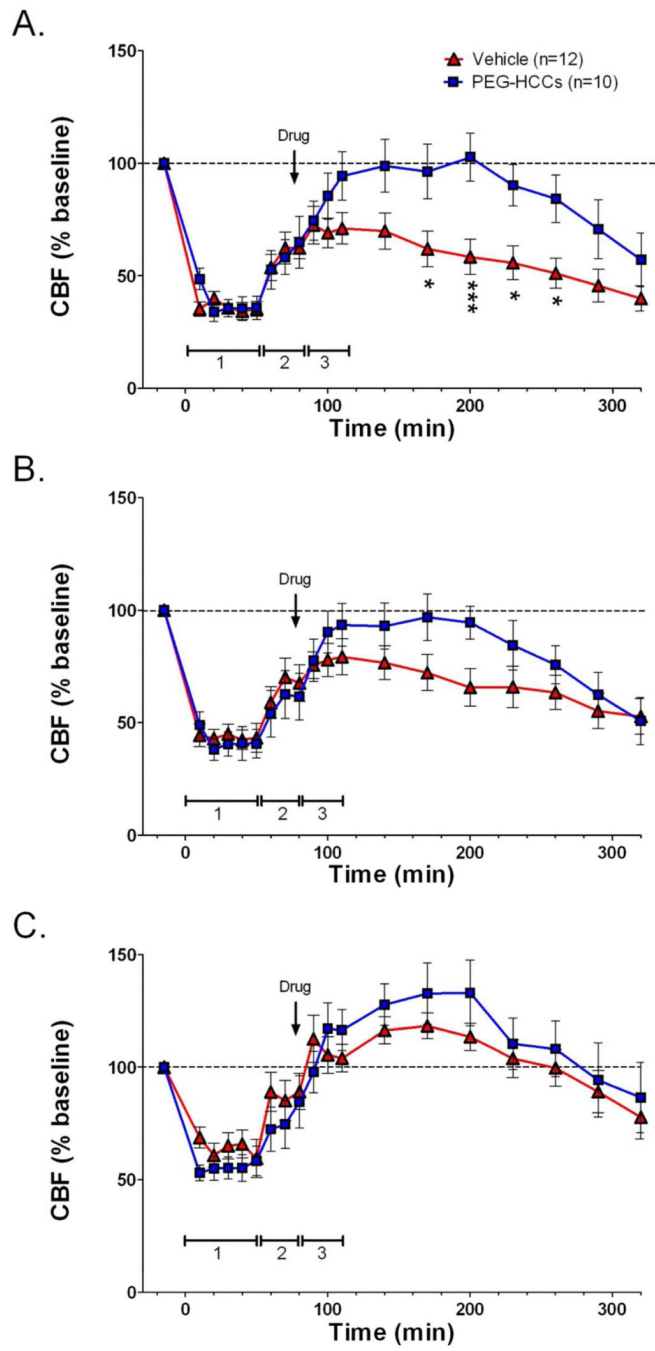


Figure 1.

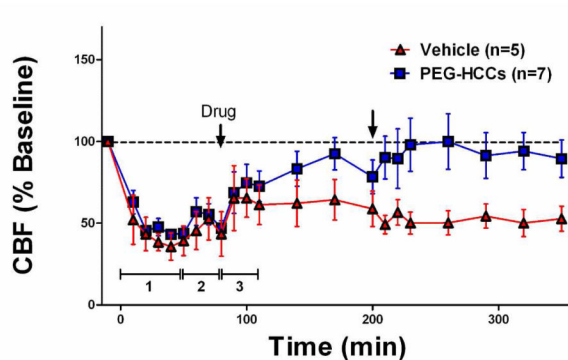
The suggested radical annihilation mechanism at a graphitic domain of the carbon particle. Two additions of RO \cdot result in the loss of two C-C pi-bonds and the formation of two new C-O sigma bonds and one new C-C pi bond, without any radical species remaining. Only one regioisomer is shown, though many others can form by resonance of the conjugated radical.

**Figure 2.**

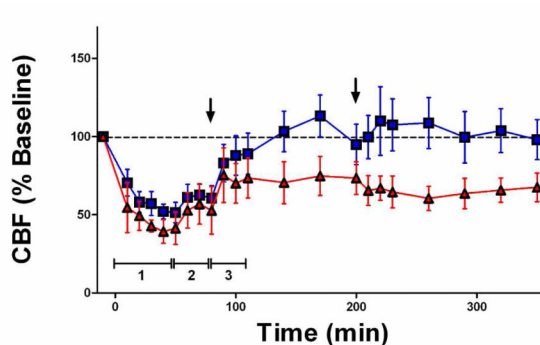
PEG-HCCs protect brain endothelial cells from oxidative stress when administered after an insult. (A) Intracellular ROS levels for b.End3 cells as determined by DHE staining and flow cytometry. The mean fluorescent intensity (MFI) of 10,000 cells/group was normalized to the group not treated with antimycin A (AntA in graphs) or DHE. Phosphate buffered saline (PBS, black bar) or antioxidant treatments (blue, green, and red solid bars) were given after antimycin A. Some antioxidants were administered prior to antimycin A (striped bars). Additional controls are shown in Figure S2. * p-value < 0.05; ** p-value < 0.01; *** p-value < 0.001 compared to bar with arrow. Results are a mean of five separate experiments. (B) Cell survival relative to control for b.End3 cells given different treatments. The cells were either cultured in the presence of PEG-HCCs, PEG-SOD or PBN alone (solid bars) or the cells were first treated with a dose of antimycin A titrated to kill 30% of the cells followed by treatment with PEG-HCCs, PEG-SOD or PBN (striped bars). Results are a mean of seven separate experiments. Error bars are s.e.m. ANOVA with Bonferroni post test was used to calculate statistics. * p-value < 0.05.



D.



E.



F.

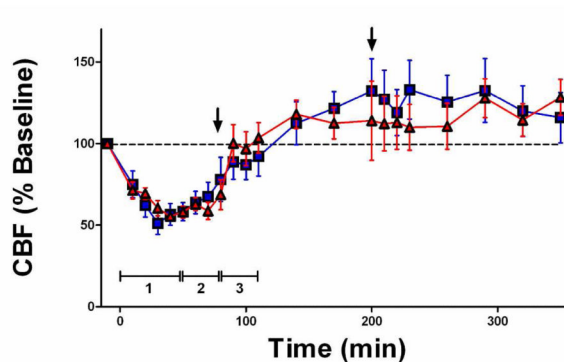


Figure 3. PEG-HCC treatment rapidly improves CBF in the injured cortex in rats with TBI plus hypotension after a single dose and two sequential doses. Laser Doppler was used to measure CBF given as a percent of the baseline (pre-injury) CBF. Relative CBF below 100 (dashed line) indicate low CBF. Relative CBF after a single drug dose (arrow) administered during the “hospital phase” in the (A) injured cortex (B) peri-lesional cortex, and (C) contralateral cortex; the effect of sequential dosing in a second set of rats treated with drug during the “hospital phase” and again 2 h later (arrows) are shown in (D) injured cortex (E) peri-lesional cortex, and (F) contralateral cortex. Drugs (PEG-HCC or PBS vehicle) were given where indicated. Time 0 min indicates when the TBI was performed. Phase 1 = TBI

+hypotension; Phase 2 = saline during “ambulatory phase”; Phase 3 = vehicle or PEG-HCC treatment and blood reinfusion during “hospital phase”. Error bars are S.E.M. Repeated measures ANOVA with Bonferroni post test was used to calculate statistics. * p-value <0.05 and *** p-value <0.01 for vehicle (red) compared to PEG-HCCs (blue). Note that 100% of CBF is considered “normal”. Approximately 50% and 150% are considered low and high cerebral blood flow, respectively.

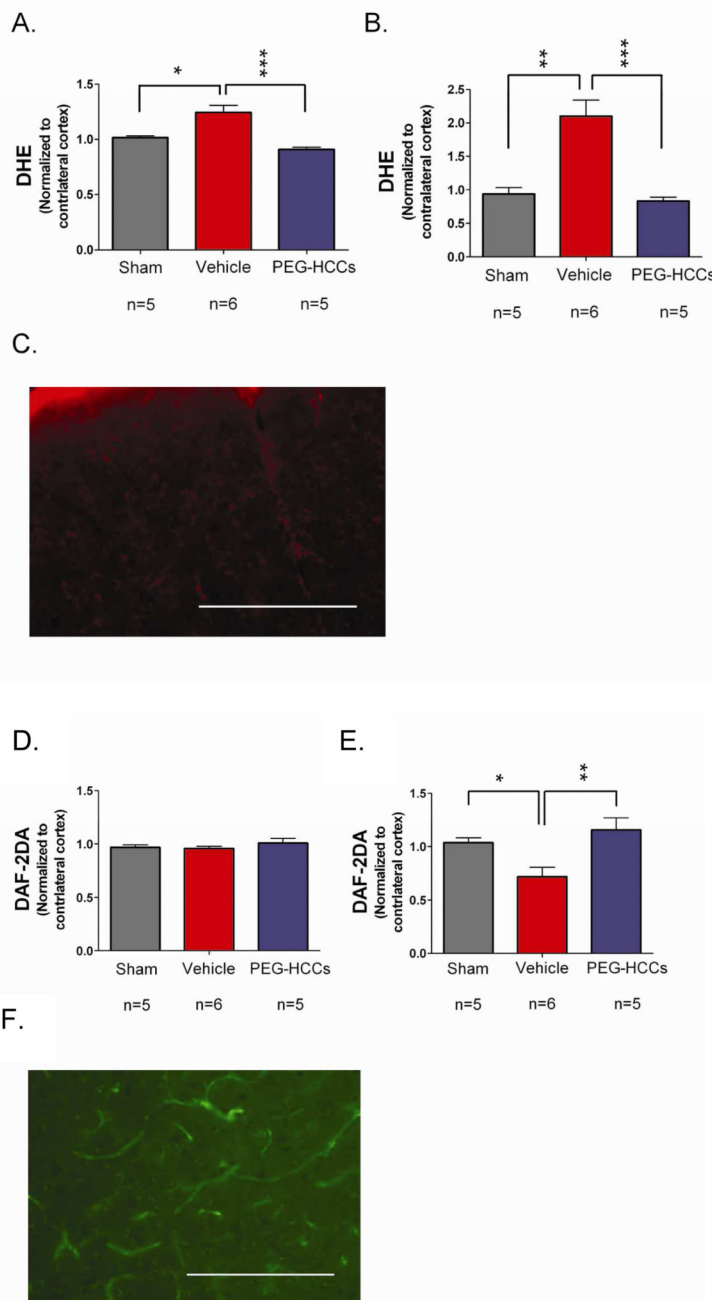


Figure 4. Fluorescence after systemic injection of radical-sensitive dyes measured in the brain and vasculature following TBI. DHE levels (proportional to SO and oxidative radicals) in the (A) brain parenchyma (cortex) and (B) blood vessels of sham (no TBI) surgery rats or rats with TBI + hypotension with vehicle or PEG-HCC treatment. The ipsilateral cortex (brain hemisphere with TBI) was normalized to the contralateral cortex. PEG-HCC treatment was able to reduce DHE staining (blue column) compared to vehicle treatment (red column), with a larger magnitude of effect seen in the blood vessels than the brain parenchyma, suggesting that the cerebrovascular is likely the site of major dysfunction in the TBI model. (C) Microscopy of DHE staining (red) in the injured cortex; scale bar = 200 μm showing the

prominent fluorescence in vascular structures (long thin structures). DAF-2DA levels (indicative of NO levels) are shown in (D) for the brain parenchyma (cortex) and (E) blood vessels of sham surgery rats or rats with TBI + hypotension with vehicle or PEG-HCCs treatment. (F) Microscopy of DAF-2DA staining (green) in the injured cortex. NO-related fluorescence was reduced following TBI and restored to levels comparable to the sham-treated animals. NO is important for vasodilation and increased CBF, therefore, increased DAF-2DA staining with PEG-HCC treatment correlates well with the improved CBF from Figure 3. Both DHE and DAF-2DA fluorescence was normalized in each animal to the contralateral cortex to account for minor differences in dye administration and circulation times. For all data in this Figure, error bars are S.E.M. D'Agostino-Pearson normality test was used on data and no groups had a p-value <0.05. ANOVA with Bonferroni post test was used to calculate statistics. * p-value < 0.05; ** p-value < 0.01; *** p-value < 0.001. N=5-6 animals/group with 10 brain sections analyzed per animal. Scale bar = 200 μ m.

Table 1

Injury Model

Phase 1 Injury and hemorrhage (50 min)	Phase 2 Prehospital-ambulance (30 min)	Phase 3 Definitive-hospital (30 min)	Phase 4 Test outcome (6 h)
<ul style="list-style-type: none"> •Ventilate (air) •Mild TBI •Withdraw blood to MAP 40 mm Hg 	<ul style="list-style-type: none"> • Ventilate (air) • Initial resuscitation-saline MAP 50 mm Hg 	<ul style="list-style-type: none"> • Give drug • Ventilate with 100% oxygen • Reinfuse blood • Saline to MAP 60 mm Hg 	<ul style="list-style-type: none"> • 0-6 h Monitor cerebral hemodynamics • 6 h Determine SO and NO levels